Received: 30 December 2021 | Revised: 26 January 2022 | Accepted: 18 February 2022

DOI: 10.1002/biot.202100712

Biotechnology Journal

RESEARCH ARTICLE

Short-chain alcohols inactivate an immobilized industrial lipase through two different mechanisms

Marco Mangiagalli[1] | **Diletta Ami**[1] | **Marcella de Divitiis**[1] | **Stefania Brocca**[1] | **Tiziano Catelani**[2] | **Antonino Natalello**[1] | **Marina Lotti**[1]

[1]Department of Biotechnology and Biosciences, University of Milano-Bicocca, Milan, Italy

[2]Microscopy Facility, University of Milano-Bicocca, Milan 20126, Italy

Correspondence
Antonino Natalello and Marina Lotti, Department of Biotechnology and Biosciences, University of Milano-Bicocca, Piazza della Scienza 2, 20126 Milan, Italy.
Email: antonino.natalello@unimib.it and marina.lotti@unimib.it

Abstract

Broadly used in biocatalysis as acyl acceptors or (co)-solvents, short-chain alcohols often cause irreversible loss of enzyme activity. Understanding the mechanisms of inactivation is a necessary step toward the optimization of biocatalytic reactions and the design of enzyme-based sustainable processes. The functional and structural responses of an immobilized enzyme, Novozym 435 (N-435), exposed to methanol, ethanol, and tert-butanol, are explored in this work. N-435 consists of *Candida antarctica* lipase B (CALB) adsorbed on polymethacrylate beads and finds application in a variety of processes involving the presence of short-chain alcohols. The nature of the N-435 material required the development of an ad hoc method of structural analysis, based on Fourier transform infrared microspectroscopy, which was complemented by catalytic activity assays and by morphological observation by transmission electron microscopy. The inactivation of N-435 was found to be highly dependent on alcohol concentration and occurs through two different mechanisms. Short-chain alcohols induce conformational changes leading to CALB aggregation, which is only partially prevented by immobilization. Moreover, alcohol modifies the texture of the solid support promoting the enzyme release. Overall, knowledge of the molecular mechanisms underlying N-435 inactivation induced by short-chain alcohols promises to overcome the limitations that usually occur during industrial processes.

KEYWORDS
biocatalysis, *Candida antarctica* lipase B, enzyme inactivation, Novozym 435, protein aggregation

1 | INTRODUCTION

The design of sustainable, effective, and economically convenient chemical processes is one of the main goals of green chemistry. Enzymatic biocatalysis allows the application of mild and sustainable conditions even on an industrial scale, improving the yields and reducing the number of reaction steps required and the production of waste.[1–3] Generally, synthetic reactions need anhydrous or low water conditions, and in this context the search for enzymes active in non-conventional (or non-aqueous) media is steadily increasing.[4] The use of non-conventional media promotes condensation reactions by limiting unwanted water-dependent reactions. Moreover, the solubil-

Abbreviations: ATR, attenuated total reflection; CALB, *Candida antarctica* lipase B; EtOH, ethanol; FTIR, Fourier transform infrared; MeOH, methanol; micro-FTIR, Fourier transform infrared microspectroscopy; N-435, Novozym 435; *p*NPO, *p*-nitrophenyl octanoate; tBuOH, tert-butanol; TEM, transmission electron microscopy

ity of hydrophobic substrates and the chemo-, regio-, and enantioselectivity of enzymes are often increased.[4–7] It has been reported that in some cases nonconventional media can impair enzyme activity and stability.[8–10] Enzyme inactivation can be irreversible, that is, due to protein denaturation and aggregation, or reversible, due to competition between the solvent and substrate molecules to bind the active site.[8,11] Immobilization of the biocatalyst is one of the strategies used to counteract the adverse effects of solvents, and often provides additional advantages, for example it might contribute to improve relevant biochemical features such as enzyme stability, selectivity, and specificity.[12,13] Among immobilized industrial enzymes, Novozym 435 (N-435) is the biocatalyst most widely used in fine chemistry, polymer synthesis and modification, glycerides modification and biodiesel production.[14] In this formulation, the *Candida antarctica* lipase B (CALB) is immobilized by interfacial activation on a Lewatit VP OC 1600 macroporous support.[15] The exploitation of N-435 was not compromised by the reduction of the catalytic activity triggered by solvent-induced support alteration[14] and/or by hydrophilic molecules such as water and glycerin.[16] These observations point out that the interaction between solvents and N-435 is a key parameter. Nonetheless, only a few seminal works investigated about the impact of solvents on the structure and activity of immobilized CALB.[17–19]

In this work, we analyze in detail the effects of short-chain alcohols (methanol – MeOH; ethanol – EtOH – and tert-butanol – tBuOH) of particular interest in biocatalysis because they can be used both as acyl acceptors and as a (co)-solvents in synthetic reactions such as the production of biodiesel.[17–23] Our results indicate that alcohols at high concentration inactivate N-435 through the formation of protein aggregates and by the enzyme release from the solid support.

2 | EXPERIMENTAL SECTION

2.1 | Chemicals

Short-chain alcohols (MeOH, EtOH, and tBuOH) at analytical grade (purity > 99.9%), N-435, the materials for hydrolytic activity assay (Triton X-100 and *p*-nitrophenyl octanoate – *p*NPO) and transesterification reactions (triolein) were purchased from Merck (Merck Darmstadt, Germany).

2.2 | Effects of short-chain alcohols on N-435

To study the effect of MeOH, EtOH, and tBuOH, 20 mg of N-435 were incubated in milliQ water, in the absence and in the presence of 15%, 45%, and 90% v/v of alcohol (throughout the text we omit to specify v/v), in a final volume of 150 μl, for 24 h, at 37°C, under orbital motion at 500 rpm in a thermal shaker (Eppendorf, Hamburg, Germany). Supernatants were collected to evaluate the CALB release (see Section 2.9), and the N-435 beads were lyophilized in a freeze-dryer (ScanVac, Analytical Control De Mori, Milano, Italy) for 1 h to completely remove traces of water and alcohol that could affect the activity of CALB. As a negative control, 20 mg of Lewatit VP OC 1600 resin were treated as N-435. For each condition, lyophilized N-435 was divided into three different aliquots for hydrolytic assay (≈2 mg), transesterification reaction (≈12 mg), and micro-FTIR analysis (≈1 mg). Aliquots of 1 mg of lyophilized N-435 were exposed to 0% and 90% alcohols, and then analyzed by transmission electron microscopy (TEM).

2.3 | Effects of short-chain alcohols on free CALB

Free CALB was recombinantly produced in *Escherichia coli* cells and purified from the culture supernatant as described in Mangiagalli et al.[24] Purified CALB was lyophilized in a freeze-dryer and stored at 4°C. Lyophilized CALB was resuspended at the concentration of 1.5 mg ml^{-1} in sodium phosphate buffer 10 mM, pH 7, in the absence and in the presence of 15%, 45%, and 90% alcohols. Samples were centrifuged for 5 min at 10,000 *g*; the supernatant was filtered using a 0.22-μm filter (Euroclone, Pero, Italy), transferred to a clean tube and incubated at 25°C for 24 h. At the end of incubation, several aliquots from each sample were withdrawn and analyzed to assess the effects of alcohols on hydrolytic activity, solubility, and secondary structure of CALB.

2.4 | Hydrolytic activity assays

The hydrolytic activity of N-435 and free CALB was evaluated on *p*NPO as a substrate. Reactions containing free CALB were carried out at 25°C in 10 mM Tris-Cl pH 8, 1% Triton X-100 and followed in continuous mode for 3 min by measuring the increase in absorbance at 410 nm with a JASCO V-770 UV/NIR spectrophotometer (JASCO Europe, Cremella, Italy). Lyophilized N-435 was added to the substrate solution and incubated at 25°C, at 100 rpm mixing speed in a thermal shaker (Eppendorf, Hamburg, Germany). At the end of the incubation time, the reaction was heated at 95°C for 2 min to stop it. Once the N-435 beads were sedimented, the supernatant was recovered, and its absorbance measured at 405 nm. The hydrolytic activity of N-435 was normalized using the following equation:

$$Specific\ activity\ (a.u./mg) = \frac{O.D.410\ nm/\ 3\ min}{mg\ of\ N-435} \quad (1)$$

Activity measured after incubation in the absence of alcohol was considered to be 100%.

2.5 | Transesterification activity assays

The transesterification activity of N-435 was determined in a mixture containing triolein (0.388 mg) and MeOH (42.7 mg) in a molar ratio 1:3. Reactions were incubated at 37°C and mixed at 500 rpm for 48 h in a thermal shaker (Eppendorf, Hamburg, Germany). The methyl ester produced was quantified using FTIR spectroscopy as described in Natalello et al.[25] Briefly, 5 μl of the organic phase were deposited onto the diamond, single reflection, attenuated total reflection (ATR) device

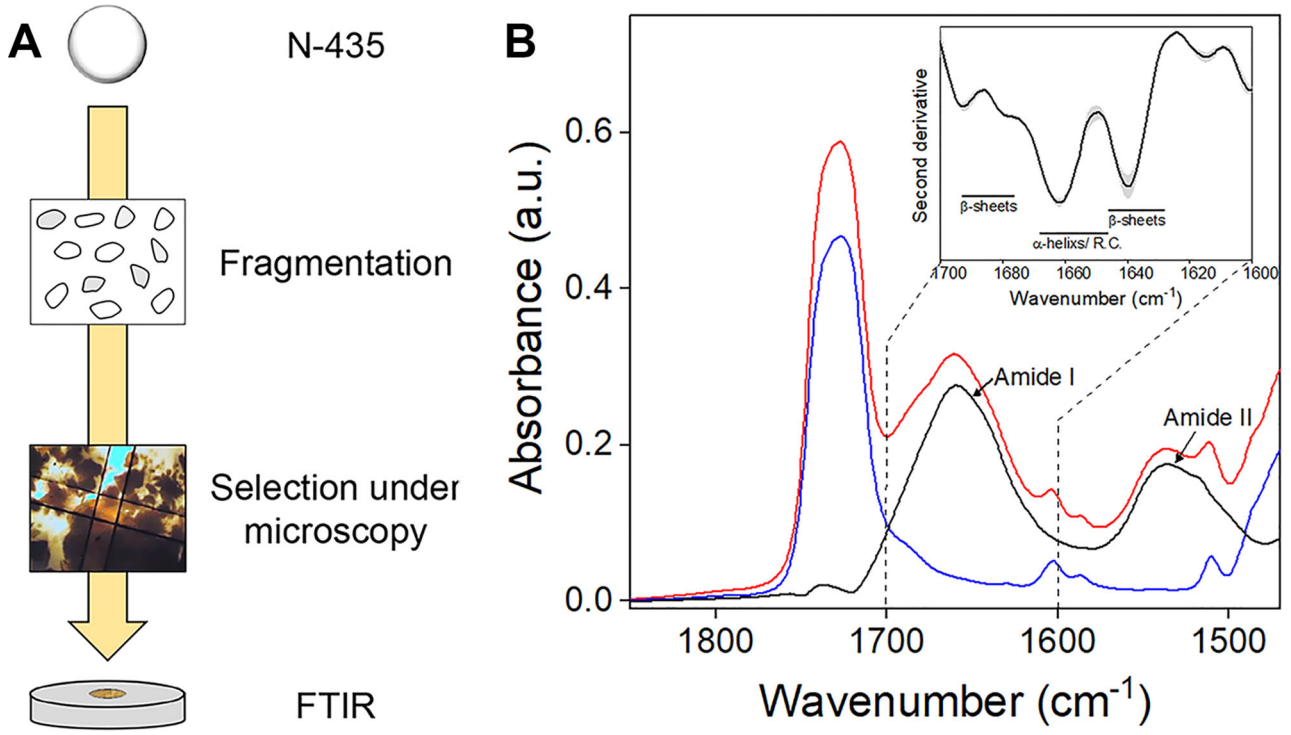

FIGURE 1 Micro-FTIR of immobilized CALB. (A) Scheme of the method used to analyze immobilized CALB. N-435 beads were fragmented between two BaF_2 windows; fragments were visually inspected to select those suitable for micro-FTIR analyses. (B) FTIR spectra of N-435 (red line), Lewatit VP OC 1600 matrix (blue line), and CALB (black line). The latter was obtained by subtracting the Lewatit VP OC spectrum from the N-435 one. The inset shows the second derivative spectrum in the amide I band range for a subtraction spectrum obtained by averaging 8 spectra. The shadowed area refers to the standard deviation of the data.

(Quest Specac, UK). The absorption spectra were collected by a Varian 670-IR spectrometer (Varian, Australia Pty Ltd., Mulgrave VIC, Australia) equipped with a nitrogen-cooled Mercury Cadmium Telluride (MCT) detector, under the following conditions: 2 cm^{-1} spectral resolution, 25 kHz scan speed, 256 scan coadditions, triangular apodization. The second derivative spectra were obtained after the Savitsky-Golay smoothing of the absorption spectra, using the Resolutions-Pro software (Varian Australia). The methyl ester content was then determined from the peak intensity at 1435 cm^{-1} in the second derivative spectra.[25]

The transesterification activity of N-435 was normalized using the following equation:

$$Specific\ activity\ (\%ME/mg) = \frac{\%\ Methyl\ ester}{mg\ of\ N-435} \quad (2)$$

Activity measured after incubation in the absence of alcohol was considered to be 100%.

2.6 | Fourier transform infrared microspectroscopy (micro-FTIR) analyses

To study the secondary structure of immobilized CALB, N-435 beads were deposited on an infrared-transparent BaF_2 window and crushed by applying a second BaF_2 window (Figure 1). Bead bits were then measured in transmission mode by an infrared microscope Varian 610-IR coupled to the infrared spectrometer Varian 670-IR (Varian, Australia Pty Ltd., Mulgrave VIC, Australia) and equipped with an MCT detector. The variable microscope aperture was adjusted to ≈100 μm × 100 μm and the following conditions were employed: 2 cm^{-1} spectral resolution, 25 kHz scan speed, 512 scan coadditions, triangular apodization. The absorption spectrum of the immobilized proteins was obtained by subtracting the spectrum of Lewatit VP OC 1600 resin (Lanxess, Koln, Germany), measured under the same experimental conditions, from the spectrum of N-435 beads. In particular, the following resin peaks were employed to optimize subtraction: ≈1730, ≈1603, and ≈1587 cm^{-1}. When necessary, spectra were corrected for vapor absorption. The second derivative spectra were obtained after the Savitsky-Golay smoothing of the absorption spectra, using Resolutions Pro Software (Varian Australia). For the characterization of free CALB secondary structure, 2–3 μl of protein were deposited on a BaF_2 support and measured after solvent evaporation, following the same experimental conditions described above.

2.7 | Solubility assay

The solubility of free CALB after exposure to alcohol was assessed by SDS-PAGE. After incubation with alcohol, samples (total protein, 40 μl) were centrifuged at 4°C for 10 min at 10,000 *g*. An equal volume (10 μl)

of supernatant (soluble proteins) and total protein from each sample was analyzed on 14% SDS-PAGE. The densitometric volume of the protein band was determined with Image Lab software (Bio-Rad, California, USA). At each condition, relative solubility was calculated with reference to total protein.

2.8 | TEM analysis

N-435 beads were sectioned in 150-nm slices using an ultramicrotome (Reichert-Jung UltracutE) equipped with Diatome diamond knives (Diatome, Nidau, Switzerland), and sections were mounted on 200-mesh carbon-coated copper grids.

TEM imaging was performed with a Jeol JEM 2100Plus (JEOL, Akishima, Tokio, Japan) 200-kV electron microscope equipped with a Gatan Rio9 (Gatan, Pleasanton, CA, USA) 9-megapixel complementary metal oxide semiconductor (CMOS) camera.

2.9 | Assessment of CALB release from the solid support

The release of CALB from the solid support was assessed by Bradford protein assay, hydrolytic activity assay and FTIR analysis of the supernatants collected after N-435 exposure to alcohol (see Section 2.2). The amount of CALB in the supernatant was determined by the Bradford protein assay (Bio-Rad, California, USA) using serum albumin as the standard. The hydrolytic activity was measured using *p*NPO as a substrate, as described in Section 2.4. An equal volume (≈90 μl) of supernatant from each sample, including the negative control, was lyophilized, resuspended in 4 μl of water and analyzed by ATR-FTIR spectroscopy. Two microliters of these samples were deposited on the diamond, single reflection, ATR device (Quest Specac, UK) and the spectrum was collected after solvent evaporation, under the conditions described in Section 2.5.

2.10 | Statistical analysis

All the experiments were repeated six times. Statistical analysis was performed using OriginPro 2020 (OriginLab Corporation, Northampton, USA). *p*-values were determined by using an unpaired two-tailed *t*-test. Second derivative spectra of the amide I band region were obtained by averaging at least 8 spectra for each condition.

3 | RESULTS

To study the secondary structure of N-435 and monitor alcohol induced changes, we developed a method based on micro-FTIR, which allows overcoming the interference of the solid support in the spectral regions of interest[26,27] (Figure 1A). N-435 beads are fragmented between two BaF_2 windows, and the fragments are visually inspected by a microscope to select those of thickness suitable for micro-FTIR analyses. Among them, spectra were collected from fragments characterized by high protein absorption. Compared to a previously published procedure,[26] our approach allows direct characterization of immobilized CALB, avoiding the use of synchrotron light and inclusion of beads in paraffin wax. The FTIR spectrum of CALB (in black in Figure 1B) was obtained by subtracting from the N-435 spectrum (in red) that of Lewatit VP OC 1600 resin (in blue). The resulting spectrum displays well resolved amide I (C═O stretching) and amide II (C—N stretching and N—H bending) bands, both due to the vibrations of the peptide bond.[28,29] The second derivative spectrum of CALB in the amide I region shows two main peaks at 1662 cm^{-1} assigned to α-helices (with possible contributions of random coils) and at 1640 cm^{-1}, assigned to native β-sheet structures. These spectral components were found in the FTIR spectra of free[24] (black line in Figure 4B and Figure S1) and immobilized CALB[26] and are consistent with the α/β fold of the protein.[30] Although our method does not provide information on the spatial distribution of the enzyme on the solid support,[26] it proved useful for studying the secondary structure of immobilized CALB and was applied to monitor the structural changes induced by short-chain alcohols.

3.1 | Effects of short-chain alcohols on CALB

The effects of MeOH and EtOH on the structure and function of lipases is of great interest due to their use as acyl acceptors in enzymatic synthesis reactions,[8,17–19] as MeOH is widely used in biodiesel production, although it is a competitive inhibitor of free CALB,[24,31–34] and EtOH is of growing relevance in renewable process design.[35] Nonetheless, their effects on N-435 are still unclear and unexplored. In the absence of alcohol, N-435 shows a specific hydrolytic activity of 1.61 ± 0.12 au mg^{-1} and a specific transesterification activity of 6.42 ± 0.49%$_{ME}$/mg, both taken as 100% of relative activity in Figure 2. At 15% MeOH, the relative activity in terms of hydrolysis and transesterification are 74.41 ± 6.93% and 79.92 ± 4.62%, respectively (Figure 2A and B). Upon incubation in 45% and 90% MeOH, the relative activities of N-435 drop to 49.82 ± 6.93% and 51.08 ± 6.41% for the hydrolysis and 46.66 ± 5.67% and 48.09 ± 7.18% for transesterification (Figure 2A and B). Micro-FTIR analysis indicates that incubation in 15% MeOH does not affect the secondary structure of immobilized CALB (Figure 3A). By contrast, incubation in 45% and 90% MeOH induces protein aggregation, as indicated mainly by the presence of a peak at ≈1625 cm^{-1}, which is typical of intermolecular β-sheet structures[28,29] (Figure 3A). A similar behavior was also observed for free CALB, although accompanied by a more remarkable loss of structure, hydrolytic activity, and solubility (Figure 4A, D, and G). Overall, immobilization seems to mitigate the detrimental effects of MeOH, in fact after exposure to 90% MeOH, the relative activity of N-435 is 2-fold higher than that observed for free CALB.

Hydrolytic and transesterification activities are slightly affected by incubation in 15% EtOH (relative activities: 77.41 ± 6.05% and 80.10 ±

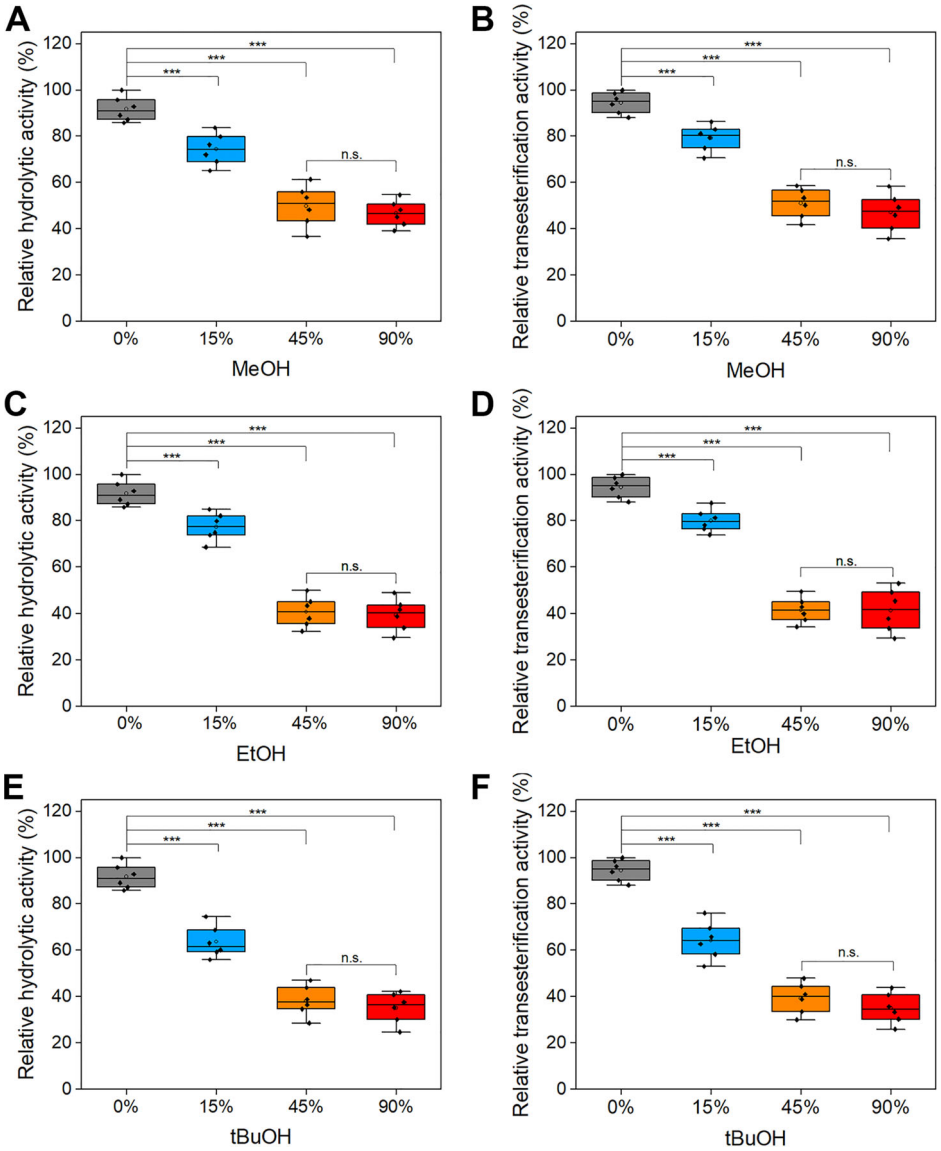

FIGURE 2 Effects of short-chain alcohols on the activity of N-435. Relative activity after exposure of N-435 to MeOH (A, B), EtOH (C, D), and tBuOH (E, F). Hydrolytic activity was measured using *p*NPO as a substrate at the concentration of 1 mM, while transesterification activity was assayed using a mixture containing MeOH and triolein in a 1:3 molar ratio. Mean values of six independent measurements are represented with error bars indicating standard deviations. Statistical analyses were performed using unpaired two-tailed Student's *t*-test, n.s.: not significant $p > 0.05$, $^{*}p < 0.05$, $^{**}p < 0.01$, $^{***}p < 0.001$.

4.94%, respectively). Higher EtOH concentrations more markedly reduce the N-435 activity in both hydrolysis (relative activities: 40.81 ± 6.55% and 39.51 ± 6.96% in 45% and 90% EtOH) and transesterification (relative activities: 41.56 ± 5.43% and 41.47 ± 9.27% in 45% and 90% EtOH) (Figure 2C and D). Similar to MeOH, higher concentrations of EtOH induce the aggregation of both immobilized and free CALB (Figures 3 and 4). Note that EtOH has a much stronger effect on free CALB, whose residual activity after treatment in 90% EtOH is 10-fold lower than that observed in N-435 (relative activity: 4% vs. 48%).

Tert-butanol is one of the most used (co)-solvents in lipase-catalyzed reactions, since this class of enzymes is not active on tertiary alcohols.[22,35] tBuOH is widely used in biodiesel production due to its ability to dissolve glycerol, which would otherwise accumulate on the surface of N-435 beads, causing inactivation and promoting bead aggregation during the reaction.[16,21–23,36]

The effects of tBuOH on the activity and structure of immobilized CALB are more pronounced than those exerted by MeOH and EtOH. Indeed, immobilized CALB undergoes aggregation already at 15% tBuOH (Figure 3). In 90% tBuOH, the residual hydrolysis and transesterification activities are 34.03 ± 5.41% and 35.03 ± 6.04%, that is, significantly lower than those obtained with MeOH and EtOH at the same concentration. These negative effects were also observed on free CALB (Figure 4), which completely loses its activity and solubility in the presence of 90% tBuOH (Figure 4C, F, and I). Interestingly, after exposure to 15% tBuOH, free CALB retains its activity, solubility and secondary structure (Figure 4C, F, and I).

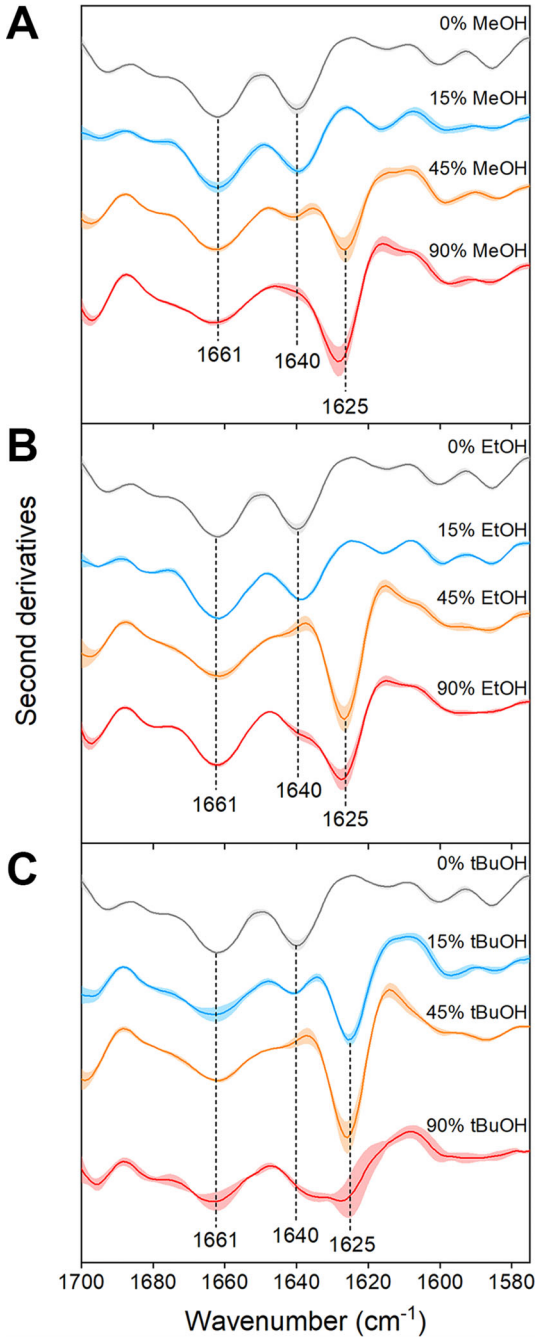

FIGURE 3 Effects of short-chain alcohols on the secondary structure of N-435. Micro-FTIR spectra were collected after exposure to MeOH (A), EtOH (B), and tBuOH (C). Second derivative spectra of the amide I band region were obtained by averaging at least 8 spectra for each condition. The shadowed area refers to the standard deviation of the data. Peak assignment is reported in Table S1.

3.2 | Effects of short-chain alcohols on CALB release from the solid support

Our results indicate that in the presence of the tested alcohols, N-435 undergoes inactivation by aggregation, to varying degrees depending on the alcohol's chemical-physical properties and concentration. At this point, we wondered if the inactivation of N-435 was entirely ascribable to aggregation of the enzyme in situ, or whether the alcohol may also induce release of CALB from its support.

To monitor the release of CALB from the resin, N-435 beads were exposed to alcohol and the supernatants were collected and analyzed. The amount of released CALB was determined by the Bradford assay (Figure 5A–C). Under all conditions tested, alcohol causes a progressive release of CALB, with more pronounced effects of tBuOH and EtOH. FTIR absorption spectra of lyophilized supernatants show the presence of two main components, corresponding to the protein signal (peaks of amide I and amide II) and the matrix signal (Figures 5D–F and S2). We observed that the amide I and II bands are better resolved at high alcohol concentrations, indicating an increase in protein concentration, in agreement with the Bradford assay. Analysis of second derivatives of amide I band obtained upon treatment with 45% and 90% alcohol indicates that the released protein is either denatured or forms aggregates, with tBuOH showing the most remarkable effect (Figure S3). The specific activity of supernatants collected after alcohol exposure decreases as alcohol concentration increases (Figure S4), due to the progressive release of partially active CALB from its support.

The effect of 0% and 90% alcohol on the N-435 matrix was analyzed by TEM to assess possible morphological changes. The macroporous texture of the Lewatit VP OC 1600 support exposed to 90% MeOH appears remarkably compact (Figure 5G and H). In contrast, larger pores are present after incubation in tBuOH and EtOH (Figure 5I and J). The support alterations observed in this work are similar to those reported in literature, and obtained in other conditions.[18,37,38] In addition, it has been reported that the Lewatit VP OC 1600 matrix can dissolve, leading to the release of acyl donors such as benzoic acid, sorbic acid, and 2-hydroxyethyl sorbate, which are contaminants giving potentially undesired products.[39] Overall, the release of the enzyme from N-435 is suggested to depend on the conformational effects induced by the alcohol on both CALB and its support.

4 | DISCUSSION

In this work, the molecular mechanisms of N-435 inactivation induced by alcohols were studied by combining experimental data obtained by spectroscopic, biochemical, and microscopic techniques. Although this issue is of broad interest, technical difficulties due to the interference of the solid support result in a few works available on this topic.[17–19] The method presented here has the advantage of being simple, straightforward, and applicable to other non-conventional media and enzyme preparations as well.

CALB activity in organic media was proved sensitive to water content.[31,40–44] The proposed inactivation mechanism gives a prominent role to the thickness of the hydration shell whose increase results in limiting the access of the substrate to the active site.[41,43,44] In our system, N-435 samples were freeze-dried after incubation to completely remove traces of water and alcohols. Based on this procedure, it is reasonable to assume that N-435 inactivation is mainly due to structural effects.

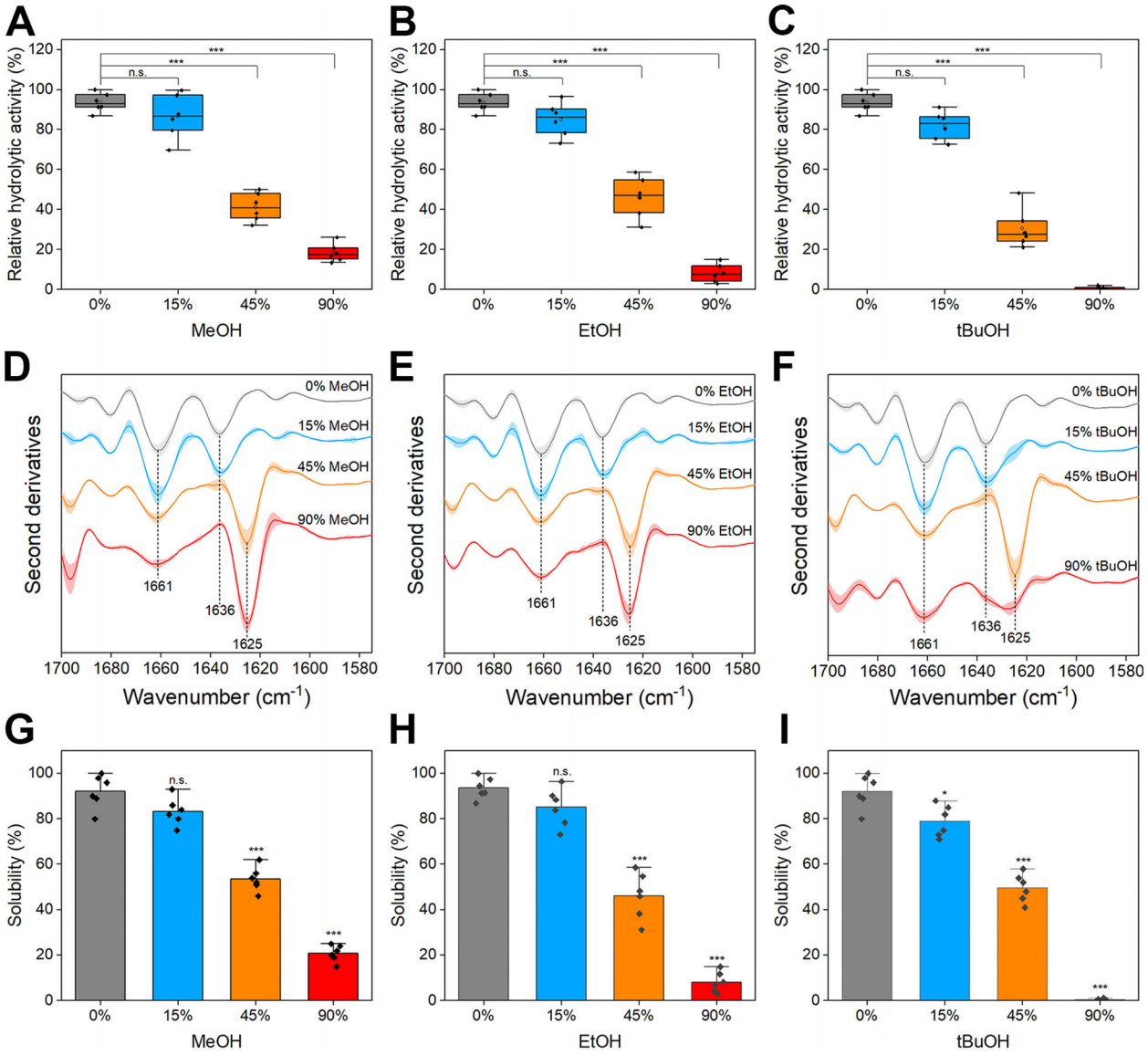

FIGURE 4 Effects of short-chain alcohols on free CALB. Relative activity after exposure of free CALB to MeOH (A), EtOH (B), and tBuOH (C). The hydrolytic activity was measured using 1 mM *p*NPO as a substrate. Micro-FTIR spectra of CALB were collected after exposure to MeOH (D), EtOH (E), and tBuOH (F). The second derivative spectra of the amide I band region were obtained by averaging at least 8 spectra for each condition. The shadowed area refers to the standard deviation of the data. Peak assignments are reported in Table S1. Solubility of free CALB after incubation in MeOH (G), EtOH (H), and tBuOH (I). Mean values of six independent measurements are represented with error bars indicating standard deviations. Statistical analyses were carried out using unpaired two-tailed Student's *t*-test, n.s.: not significant $p > 0.05$, $^{*}p < 0.05$, $^{**}p < 0.01$, $^{***}p < 0.001$.

Our results indicate that MeOH and EtOH at the highest concentrations used in this work induce the aggregation of free and immobilized CALB, causing irreversible loss of activity, whereas CALB well tolerates MeOH and EtOH up to 15%. Therefore, data highlight the importance of finding a trade-off between the alcohol concentration required by a given reaction and the enzyme performance and strengthen the stepwise addition of alcohols during the process as a possible solution to counteract the irreversible inactivation of N-435 induced by high alcohol concentrations.[36,45–47] On the other hand, the inactivation of N-435 by tBuOH is more pronounced than those induced by MeOH and EtOH and not consistent with the beneficial effect (i.e., increase of product yields) reported when tBuOH is used as a solvent in biodiesel transesterification reactions.[16,21–23,36] We cannot exclude that the glycerol produced during transesterification stabilizes CALB and prevents its aggregation, as reported for other proteins[48,49] and would hypothesize that the outcomes of tBuOH in transesterification reactions could be due to a combination of negative (i.e., inactivation of the enzyme) and positive (i.e., better dissolution of MeOH and glycerol) effects.

CALB release from the solid support, observed in the presence of tested alcohols, might be due to the weakening of the enzyme-support interactions and/or to changes of the solid support itself. The phe-

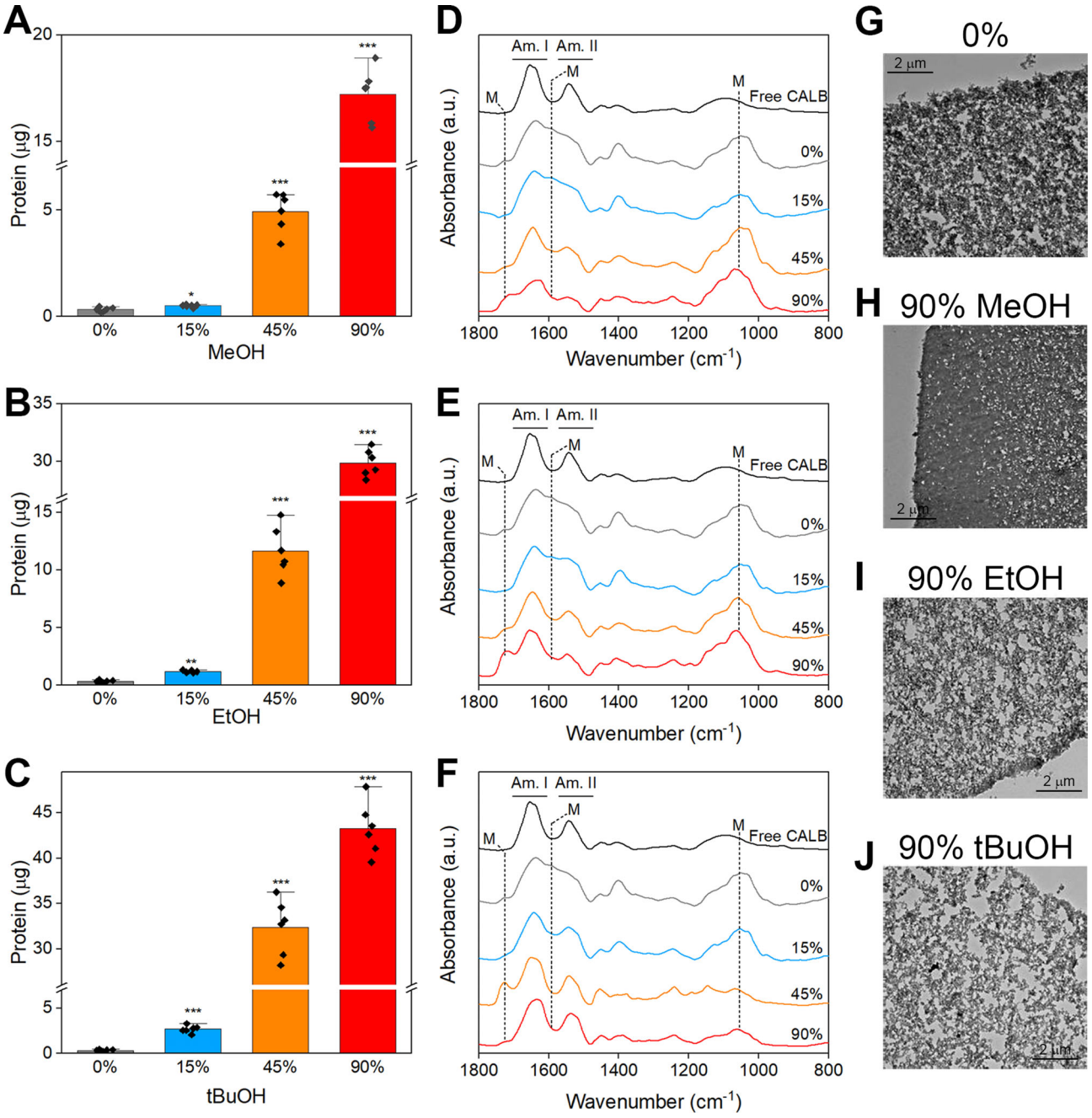

FIGURE 5 Effects of short-chain alcohols on the release of CALB from the solid support. Bradford assay (A–C). The mean values of six independent measurements are represented with error bars indicating standard deviations. Statistical analyses were carried out using unpaired two-tailed Student's *t*-test, $^{*}p < 0.05$, $^{**}p < 0.01$, $^{***}p < 0.001$. ATR-FTIR analyses (D–F) performed on lyophilized supernatants, resuspended in water, after incubation in MeOH (D), EtOH (E), and tBuOH (F). Am. I and Am. II: amide I and amide II bands; M: peaks typical of the Lewatit VP OC 1600. One of six independent experiments is shown. TEM analysis (G–J) on N-435 incubated for 24 h at 37°C in the absence and in the presence of 90% alcohols. One of three independent experiments is shown.

nomenon of enzyme leaching is commonly observed when lipases are immobilized by interfacial activation on hydrophobic support as in the case of N-435 and has to be considered with caution when planning the conditions for the use of this enzyme in industrial application.[14,45–47]

The overall scenario that can be drawn from the data reported suggests that short-chain alcohols induce inactivation of N-435 through two different mechanisms: *i)* conformational changes that induce aggregation of CALB on the surface of the solid support; *ii)* detachment of the enzyme from its support. The higher susceptibility to alcohol inactivation of free and released CALB indirectly suggests that immobilization protects the enzyme from harmful alcohols effects. On this ground, the design of biocatalytic processes should consider the complexity of the interaction between short-chain alcohols and immobilized CALB. Indeed, in addition to the inactivation mecha-

nisms described in this work there is evidence for influence of water activity,[31,40–44] competitive inhibition[24,31,32,34] and effects on the local conformational dynamics.[24,33,50,51]

In conclusion, the knowledge of the multitude of factors and mechanisms underlying enzymatic inactivation by short-chain alcohols promises to contribute to both the optimization of biocatalytic reactions and the development of new sustainable processes.

ACKNOWLEDGEMENTS

The authors acknowledge LANXESS Deutschland GmbH (Koln, Germany) for kindly providing the Lewatit VP OC 1600 matrix and the Interdepartmental Microscopy Platform of the University of Milano-Bicocca. This work was partially supported by the Sugar BEEt biorefinery for the integrated prOduction of biofUel and polyesTers (BEETOUT) project, funded by Fondazione Cariplo (2015-0375) and by Fondo di Ateneo of the University of Milano-Bicocca (2019-ATE-0457, A.N. and 2018-ATE-0320, M.L.). M.M. and A.D. benefit of a post-doctoral research fellow (Assegno di Ricerca) from the University of Milano-Bicocca.

Open access funding enabled and organized by Projekt DEAL.

CONFLICT OF INTEREST

The authors declare no commercial or financial conflict of interest.

DATA AVAILABILITY STATEMENT

The data that support the findings of this study are available from the corresponding author upon reasonable request.

ORCID

Marco Mangiagalli https://orcid.org/0000-0001-8211-165X
Antonino Natalello https://orcid.org/0000-0002-1489-272X

REFERENCES

1. Sheldon, R. A. & Woodley, J. M. (2018) Role of biocatalysis in sustainable chemistry. *Chemical Reviews 118*, 801–838. https://doi.org/10.1021/acs.chemrev.7b00203.
2. de María, P., de Gonzalo, G. & Alcántara, A. (2019) Biocatalysis as useful tool in asymmetric synthesis: An assessment of recently granted patents (2014–2019). *Catalysts 9*, 802https://doi.org/10.3390/catal9100802.
3. Wu, S., Snajdrova, R., Moore, J. C., Baldenius, K. & Bornscheuer, U. T. (2021) Biocatalysis: Enzymatic synthesis for industrial applications. *Angewandte Chemie - International Edition 60*, 88–119. https://doi.org/10.1002/anie.202006648.
4. van Schie, M. M. C. H., Spöring, J. - D., Bocola, M., Domínguez de María, P. & Rother, D. (2021) Applied biocatalysis beyond just buffers – From aqueous to unconventional media. Options and guidelines. *Green Chemical 23*, 3191–3206. https://doi.org/10.1039/D1GC00561H.
5. Kumar, A., Dhar, K., Kanwar, S. S. & Arora, P. K. (2016) Lipase catalysis in organic solvents: Advantages and applications. *Biological Procedures Online 18*, 2. https://doi.org/10.1186/s12575-016-0033-2.
6. Klibanov, A. M. (2001) Improving enzymes by using them in organic solvents. *Nature 409*, 241–246. https://doi.org/10.1038/35051719.
7. Cao, C. & Matsuda, T. (2016) Biocatalysis in organic solvents, supercritical fluids and ionic liquids, *Organic synthesis using biocatalysis* (pp. 67–97). Elsevier. https://doi.org/10.1016/B978-0-12-411518-7.00003-2.
8. Lotti, M., Pleiss, J., Valero, F. & Ferrer, P. (2018) Enzymatic production of biodiesel: Strategies to overcome methanol inactivation. *Biotechnology Journal 13*, 1700155. https://doi.org/10.1002/biot.201700155.
9. Lotti, M., Pleiss, J., Valero, F. & Ferrer, P. (2015) Effects of methanol on lipases: Molecular, kinetic and process issues in the production of biodiesel. *Biotechnology Journal 10*, 22–30. https://doi.org/10.1002/biot.201400158.
10. Serdakowski, A. L. & Dordick, J. S. (2008) Enzyme activation for organic solvents made easy. *Trends Biotechnology 26*, 48–54. https://doi.org/10.1016/j.tibtech.2007.10.007.
11. Ingenbosch, K. N., Vieyto-Nuñez, J. C., Ruiz-Blanco, Y. B., Mayer, C., Hoffmann-Jacobsen, K. & Sanchez-Garcia, E. (2022) Effect of organic solvents on the structure and activity of a minimal lipase. *Journal of Organic Chemistry Research 87*, 1669. https://doi.org/10.1021/acs.joc.1c01136.
12. Mateo, C., Palomo, J. M., Fernandez-Lorente, G., Guisan, J. M. & Fernandez-Lafuente, R. (2007) Improvement of enzyme activity, stability and selectivity via immobilization techniques. *Enzyme and Microbial Technology 40*, 1451–1463. https://doi.org/10.1016/j.enzmictec.2007.01.018.
13. Sheldon, R. A. (2007) Enzyme immobilization: The quest for optimum performance. *Advanced Synthesis and Catalysis 349*, 1289–1307. https://doi.org/10.1002/adsc.200700082.
14. Ortiz, C., Ferreira, M. L., Barbosa, O., dos Santos, J. C. S., Rodrigues, R. C., Berenguer-Murcia, Á., Briand, L. E. & Fernandez-Lafuente, R. (2019) Novozym 435: the "perfect" lipase immobilized biocatalyst? *Catalysis Science and Technology 9*, 2380–2420. https://doi.org/10.1039/C9CY00415G.
15. Johnson, C. R. & Bis, S. J. (1992) Enzymatic asymmetrization of meso-2-cycloalken-1,4-diols and their diacetates in organic and aqueous media. *Tetrahedron Letters 33*, 7287–7290. https://doi.org/10.1016/S0040-4039(00)60167-3.
16. Kuramochi, H., Maeda, K. & Kobayashi, T. (2020) Aggregation of immobilized enzyme during transesterification of triolein and methanol, and the effect of two types of aggregates on reaction yield. *Fuel 260*, 116343. https://doi.org/10.1016/j.fuel.2019.116343.
17. José, C., Bonetto, R. D., Gambaro, L. A., del, P. G., Torres, M., Foresti, M. L., Ferreira, M. L. & Briand, L. E. (2011) Investigation of the causes of deactivation–degradation of the commercial biocatalyst Novozym® 435 in ethanol and ethanol–aqueous media. *Journal of Molecular Catalysis. B, Enzymatic 71*, 95–107. https://doi.org/10.1016/j.molcatb.2011.04.004.
18. José, C. & Briand, L. E. (2009) Deactivation of NovozymÂ® 435 during the esterification of ibuprofen with ethanol: Evidences of the detrimental effect of the alcohol. *Reaction Kinetics, Mechanisms and Catalysis*. https://doi.org/10.1007/s11144-009-0103-4.
19. Toledo, M. V., José, C., Suster, C. R. L., Collins, S. E., Portela, R., Bañares, M. A. & Briand, L. E. (2021) Catalytic and molecular insights of the esterification of ibuprofen and ketoprofen with glycerol. *Molecular Catalysis 513*, 111811. https://doi.org/10.1016/j.mcat.2021.111811.
20. Kamal, Md.Z., Yedavalli, P., Deshmukh, M. V. & Rao, N. M. (2013) Lipase in aqueous-polar organic solvents: Activity, structure, and stability: lipase in organic solvents. *Protein Science 22*, 904–915. https://doi.org/10.1002/pro.2271.
21. Chen, J. - W. & Wu, W. - T. (2003) Regeneration of immobilized *Candida antarctica* lipase for transesterification. *J Bioscience & Bioengineering 95*, 466–469. https://doi.org/10.1016/S1389-1723(03)80046-4.
22. Royon, D., Daz, M., Ellenrieder, G. & Locatelli, S. (2007) Enzymatic production of biodiesel from cotton seed oil using t-butanol as a solvent. *Bioresource Technology 98*, 648–653. https://doi.org/10.1016/j.biortech.2006.02.021.
23. Soumanou, M. M. & Bornscheuer, U. T. (2003) Improvement in lipase-catalyzed synthesis of fatty acid methyl esters from sunflower oil. *Enzyme and Microbial Technology 33*, 97–103. https://doi.org/10.1016/S0141-0229(03)00090-5.

24. Mangiagalli, M., Carvalho, H., Natalello, A., Ferrario, V., Pennati, M. L., Barbiroli, A., Lotti, M., Pleiss, J. & Brocca, S. (2020) Diverse effects of aqueous polar co-solvents on *Candida antarctica* lipase B. *International Journal of Biological Macromolecules 150*, 930–940. https://doi.org/10.1016/j.ijbiomac.2020.02.145.
25. Natalello, A., Sasso, F. & Secundo, F. (2013) Enzymatic transesterification monitored by an easy-to-use Fourier transform infrared spectroscopy method. *Biotechnology Journal 8*, 133–138. https://doi.org/10.1002/biot.201200173.
26. Mei, Y., Miller, L., Gao, W. & Gross, R. A. (2003) Imaging the distribution and secondary structure of immobilized enzymes using infrared microspectroscopy. *Biomacromolecules. 4*, 70–74. https://doi.org/10.1021/bm025611t.
27. Collins, S. E., Lassalle, V. & Ferreira, M. L. (2011) FTIR-ATR characterization of free Rhizomucor Meihei Lipase (RML), lipozyme RM IM and chitosan-immobilized RML. *Journal of Molecular Catalysis. B, Enzymatic 72*, 220–228. https://doi.org/10.1016/j.molcatb.2011.06.009.
28. Barth, A. (2007) Infrared spectroscopy of proteins. *Biochimica et Biophysica Acta - Bioenergetics 1767*, 1073–1101. https://doi.org/10.1016/j.bbabio.2007.06.004.
29. Natalello, A. & Doglia, S. M. (2015) Insoluble protein assemblies characterized by fourier transform infrared spectroscopy, In E. García-Fruitós (Ed.), *Insoluble proteins* (pp. 347–369). Springer New York. https://doi.org/10.1007/978-1-4939-2205-5_20.
30. Uppenberg, J., Hansen, M. T., Patkar, S. & Jones, T. A. (1994) The sequence, crystal structure determination and refinement of two crystal forms of lipase B from Candida antarctica, *Structure 2*, 293–308. https://doi.org/10.1016/S0969-2126(00)00031-9.
31. Kulschewski, T., Sasso, F., Secundo, F., Lotti, M. & Pleiss, J. (2013) Molecular mechanism of deactivation of *C. antarctica* lipase B by methanol. *Journal of Biotechnology 168*, 462–469. https://doi.org/10.1016/j.jbiotec.2013.10.012.
32. Sasso, F., Kulschewski, T., Secundo, F., Lotti, M. & Pleiss, J. (2015) The effect of thermodynamic properties of solvent mixtures explains the difference between methanol and ethanol in *C. antarctica* lipase B catalyzed alcoholysis. *Journal of Biotechnology 214*, 1–8. https://doi.org/10.1016/j.jbiotec.2015.08.023.
33. Carvalho, H. F., Ferrario, V. & Pleiss, J. (2021) Molecular mechanism of methanol inhibition in calb-catalyzed alcoholysis: Analyzing molecular dynamics simulations by a Markov state model. *Journal of Chemical Theory and Computation 17*, 6570–6582. https://doi.org/10.1021/acs.jctc.1c00559.
34. Fang, X., Zhan, Y., Yang, J. & Yu, D. (2014) A concentration-dependent effect of methanol on Candida antarctica lipase B in aqueous phase. *Journal of Molecular Catalysis. B, Enzymatic 104*, 1–7. https://doi.org/10.1016/j.molcatb.2014.03.002.
35. Fjerbaek, L., Christensen, K. V. & Norddahl, B. (2009) A review of the current state of biodiesel production using enzymatic transesterification. *Biotechnology & Bioengineering 102*, 1298–1315. https://doi.org/10.1002/bit.22256.
36. Li, L., Du, W., Liu, D., Wang, L. & Li, Z. (2006) Lipase-catalyzed transesterification of rapeseed oils for biodiesel production with a novel organic solvent as the reaction medium. *Journal of Molecular Catalysis. B, Enzymatic 43*, 58–62. https://doi.org/10.1016/j.molcatb.2006.06.012.
37. Hoogenboom, R., Becer, C. R., Guerrero-Sanchez, C., Hoeppener, S. & Schubert, U. S. (2010) Solubility and thermoresponsiveness of PMMA in alcohol-water solvent mixtures. *Australian Journal of Chemistry 63*, 1173. https://doi.org/10.1071/CH10083.
38. González-Benito, J. & Koenig, J. L. (2002) FTIR Imaging of the dissolution of polymers. 4. poly(methyl methacrylate) using a cosolvent mixture (Carbon Tetrachloride/Methanol), *Macromolecules 35*, 7361–7367. https://doi.org/10.1021/ma020401u.
39. Zhao, H. & Song, Z. (2010) Migration of reactive trace compounds from NovozymÂ® 435 into organic solvents and ionic liquids. *Biochemical Engineering Journal 49*, 113–118. https://doi.org/10.1016/j.bej.2009.12.004.
40. Lee, S. B. & Kim, K.-J. (1995) Effect of water activity on enzyme hydration and enzyme reaction rate in organic solvents. *Journal of Fermentation and Bioengineering 79*, 473–478. https://doi.org/10.1016/0922-338X(95)91264-6.
41. Dutta Banik, S., Nordblad, M., Woodley, J. & Peters, G. (2017) Effect of water clustering on the activity of candida antarctica lipase b in organic medium. *Catalysts 7*, 227. https://doi.org/10.3390/catal7080227.
42. Secundo, F., Carrea, G., Soregaroli, C., Varinelli, D. & Morrone, R. (2001) Activity of different *Candida antarctica* lipase B formulations in organic solvents. *Biotechnology & Bioengineering 73*, 157–163. https://doi.org/10.1002/bit.1047.
43. Dutta Banik, S., Nordblad, M., Woodley, J. M. & Peters, G. H. (2016) A Correlation between the activity of *Candida antarctica* lipase B and differences in binding free energies of organic solvent and substrate. *ACS Catalysis 6*, 6350–6361. https://doi.org/10.1021/acscatal.6b02073.
44. Wedberg, R., Abildskov, J. & Peters, G. H. (2012) Protein dynamics in organic media at varying water activity studied by molecular dynamics simulation. *Journal of Physics & Chemistry B 116*, 2575–2585. https://doi.org/10.1021/jp211054u.
45. Shimada, Y., Watanabe, Y., Samukawa, T., Sugihara, A., Noda, H., Fukuda, H. & Tominaga, Y. (1999) Conversion of vegetable oil to biodiesel using immobilized *Candida antarctica* lipase. *Journal of the American Oil Chemists' Society 76*, 789–793. https://doi.org/10.1007/s11746-999-0067-6.
46. Martani, F., Maestroni, L., Torchio, M., Ami, D., Natalello, A., Lotti, M., Porro, D. & Branduardi, P. (2020) Conversion of sugar beet residues into lipids by Lipomyces starkeyi for biodiesel production. *Microbial Cell Factories 19*, 204. https://doi.org/10.1186/s12934-020-01467-1.
47. Watanabe, Y., Shimada, Y., Sugihara, A., Noda, H., Fukuda, H. & Tominaga, Y. (2000) Continuous production of biodiesel fuel from vegetable oil using immobilized *Candida antarctica* lipase. *Journal of the American Oil Chemists' Society 77*, 355–360. https://doi.org/10.1007/s11746-000-0058-9.
48. Vagenende, V., Yap, M. G. S. & Trout, B. L. (2009) Mechanisms of protein stabilization and prevention of protein aggregation by glycerol. *Biochemistry 48*, 11084–11096. https://doi.org/10.1021/bi900649t.
49. Gekko, K. & Timasheff, S. N. (1981) Mechanism of protein stabilization by glycerol: Preferential hydration in glycerol-water mixtures. *Biochemistry 20*, 4667–4676. https://doi.org/10.1021/bi00519a023.
50. Trodler, P. & Pleiss, J. (2008) Modeling structure and flexibility of *Candida antarctica* lipase B in organic solvents. *BMC Structural Biology 8*, 9. https://doi.org/10.1186/1472-6807-8-9.
51. Ganjalikhany, M. R., Ranjbar, B., Taghavi, A. H. & Moghadam, T. T (2012) Functional motions of *Candida antarctica* lipase B: A survey through open-close conformations. *PLoS One 7*, e40327. https://doi.org/10.1371/journal.pone.0040327.

SUPPORTING INFORMATION

Additional supporting information may be found in the online version of the article at the publisher's website.

How to cite this article: Mangiagalli, M., Ami, D., de Divitiis, M., Brocca, S., Catelani, T., Natalello, A., & Lotti, M. (2022). Short-chain alcohols inactivate an immobilized industrial lipase through two different mechanisms. *Biotechnology Journal*, 1–10. https://doi.org/10.1002/biot.202100712